JOURNAL OF PHYSICAL ORGANIC CHEMISTRY
J. Phys. Org. Chem. 2006; **19:** 10–17
Published online 21 September 2005 in Wiley InterScience (www.interscience.wiley.com). DOI: 10.1002/poc.992

Evaluation of the aromatic contribution to the energy of periodic lattices

Jean-Paul Malrieu[1] and Vincent Robert[2]*

[1]Laboratoire de Physique Quantique, IRSAMC/UMR5626, Université Paul Sabatier, 118 route de Narbonne, F-31062 Toulouse Cedex 4, France
[2]Laboratoire de Chimie, UMR 5182 Ecole Normale Supérieure de Lyon, 46 allée d'Italie, 69364 Lyon Cedex 07, France

Received 10 June 2005; revised 26 July 2005; accepted 2 August 2005

ABSTRACT: The cohesive energy of an infinite two-dimensional lattice such as graphite is governed by the connectivity (number of bonds per atom) of the graph and by the cyclic effects. We propose to define the aromatic contribution to the cohesive energy of a specific lattice as the difference between the exact cohesive energy and that of an ideal dendrimer of the same connectivity. Direct evaluation of the cyclic contributions are possible starting from fully localized zeroth-order wavefunctions and using an order-by-order perturbative expansion or a recently proposed coupled-cluster formalism, which allow one to identify clearly the energetic role of the ring currents. Copyright © 2005 John Wiley & Sons, Ltd.
Supplementary electronic material for this paper is available in Wiley Interscience at http://www.interscience.wiley.com/jpages/0894-3230/suppmat/

KEYWORDS: periodic lattice energy; aromatics; coupled cluster; graphite

INTRODUCTION

The concepts of aromaticity and antiaromaticity play an important role in chemistry. Several criteria, including bond length equalization, chemical reactivity and physical properties (e.g. stabilization energy), have been introduced to rationalize these definitions. Based on Hückel's milestone papers,[1] specific stabilities have been attributed to the presence of six- (or ten-) membered rings with six (or ten) electrons. Conversely, the lack of stability has been sought in four- (or eight-) membered rings occupied by four (or eight) electrons. An important, although not systematic, connection was established between these energetics features and the existence of cyclic circulations of electrons along the ring, i.e. the so-called ring currents, as they manifest themselves in other observables, in particular in NMR spectroscopy. It is commonly accepted that aromatic molecules ($4n+2$ π-electrons) are characterized by unifom geometries (i.e. identical C—C distances), whereas antiaro-matic species ($4n$ π-electrons) exhibit alternating bond lengths and rather localized electronic structures. However, some antiaromatic species (e.g. the polymethinium cation $C_5H_9N_2^+$) may exhibit nearly equal C—C bond lengths. Even more surprinsingly, the highly aromatic compound tetracene exhibits bond length variations of the order of 0.1 Å. Hence, the characterization of aromaticity using these criteria may be ambiguous. Considering these limitations, it was therefore suggested that coumpounds which exhibit significantly exalted diamagnetic susceptibility are aromatic.[2] Such a definition was supported by a detailed analysis of experimental and *ab initio* data.

In fact, the magnetic properties of aromatic and antiaromatic compounds families differ significantly. In the former, a prefered flow orientation in the presence of a magnetic field generates a magnetic field in the opposite direction, resulting in an enhancement of the diamagnetic contributions. Conversely, the paramagnetic contributions arising from the mixing of the excited states with the ground state may be dominant, resulting in a net positive magnetic susceptibility.

Recently, the important factors controlling the aromatic and antiaromatic patterns have been analyzed.[3] On the basis of a valence-bond approach, the authors concluded that a fundamental difference lies in the symmetry-controlled mixing of ionic stuctures into the covalent states. In particular, the absence in the ground state of the so-called diagonal ionic structures where charges are located on opposite sites is clear evidence of the vanishing circulation of π-electrons in antiaromatic species such as cyclobutadiene. In molecules such as benzene, it has been shown that such mixing accounts for the electronic flow around the ring perimeter. On the basis of a topological analysis using the electron localization function (ELF), the separation into the σ and π contributions has been evoked to build up an aromaticity scale.[4]

From the experimental point of view, much effort has been devoted to the synthesis of conjugated molecules.

**Correspondence to:* V. Robert, Laboratoire de Chimie, UMR 5182 Ecole Normale Supérieure de Lyon, 46 allée d'ltalie, 69364 Lyon Cedex 07, France.
E-mail: vrobert@ens-lyon.fr

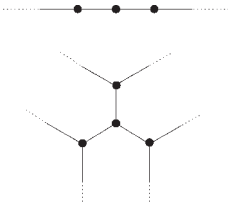

Figure 1. Schematic representation of dendrimers

Among the most challenging issues are the design of molecular wires using conjugated oligomers such as polypyrrole or polythiophene and the control of the linear (and non-linear) optical response trends.[5] The synthesis of ladder-conjugated systems was first considered as a possible strategy to avoid the Peierls instability and simultaneously reach and control low bandgaps. Following this trend, dendrimeric structures (Fig. 1) consisting of increasing branches of definite length and chemical constitution have been prepared in the last decade.[6] Clearly, the electronic and photonic applications which have been anticipated in these conjugated materials has opened up a wide perspective for theoretical investigations.

The aim of this study was to look into the importance of aromatic contributions in periodic systems. We shall concentrate mainly on the cohesive energy and leave the evaluation of other properties such as the bandgap energy for the future. Although mostly used for molecules, and particularly for conjugated hydrocarbons, the concept of aromaticity may also be applied to periodic lattices such as graphite. However, the criteria used to distinguish aromatic from antiaromatic species are controversial, as mentioned before for molecular systems. Therefore, one has first to define a reference system on which the delocalization contributions can be evaluated.

The equivalence of all atoms in such a lattice greatly simplifies the issue of the definition of a non-aromatic reference from which the strictly aromatic contributions should be defined. It will be shown from a simple derivation that the first crucial characteristic of a lattice regarding its cohesive energy is the connectivity of the graph, i.e. the number of bonds in which each atom is involved. We will then concentrate on a relevant ring-free lattices, the dendrimers of the same connectivity, to evaluate the aromatic or antiaro-matic contributions to the total energy. An analytical approach is derived in order to identify directly the energetic role of the cyclic electronic circulation around the rings which appears directly as differences to the energy contributions of the ideal dendrimeric reference. The influence of closed paths (i.e. rings) in infinite systems has already been reported using the moment method.[7]

We shall follow a constructive approach for both the periodic system and the reference dendrimer to identify the differenciated contributions and grasp their physical content in the light of the cyclic circulation. The method starts from strongly localized zeroth-order pictures and relies on a Rayleigh–Schrodinger (RS) expansion or a coupled-cluster (CC) treatment.[8] It will become apparent that the localized character of the reference function is crucial in order to obtain analytical expressions and to stress the respective role of the connectivity of the graph and the cyclic circulations of the electrons in a variety of graphs of connectivity 3 combining squares, hexagons and octagons. Emphasis will be placed on the RS expansion since the energy is built as a rational sum of order-by-order corrections. The CC evaluations based on the recently reported self-consistent perturbative equations (SCPEs)[9] will be used for control.

METHODOLOGICAL DETAILS

Step-by-step perturbative energy evaluation

Our analysis will be limited to periodic lattices where all sites are equivalent and bring one electron per site (half-filled bands). The familiar π-systems of conjugated hydrocarbons obviously fall into this class of compounds. In order to illustrate the role of the connectivity (defined as the number of nearest-neighbor atoms) in the cohesive energy, we shall consider a dendrimer of connectivity n_c. Such systems are under intense experimental investigation at present since important properties such as non-linear optics are anticipated. Dendrimers with connectivities 2 and 3 (the so-called '3-tree') are shown in Fig. 1. For $n_c = 2$, the dendrimer is a linear chain. Obviously, steric hindrance prevents the existence of such dendrimeric conjugated hydrocarbons. However, their treatment through simplified Hamiltonians such as Hubbard or Hückel is perfectly possible. In the Hückel limit, the α spin electrons move independently from the β spin electrons. Hence one can concentrate on the α part of the wavefunction which will give half of the cohesive energy. Details of the step-by-step energy corrections using the RS perturbation theory are given in the Supporting Information, available in Wiley Interscience.

Each atom is involved in a single bonding orbital i of energy t built on two atomic orbitals (AOs), whereas the corresponding antibonding MO i^* energy is $-t$. The zeroth-order determinant Φ_0 is the product of the doubly occupied bonding MOs. Hence the zeroth-order energy per bond (i.e. the zeroth-order cohesive energy) is the same for all lattices, $E_{\mathrm{coh}} = t$.

One must then introduce the delocalization between bonds which proceeds through the excitations from a bonding MO i to the nearest-neighbor (NN) antibonding MOs j^* (see Fig. 2). The resulting charge-transfer

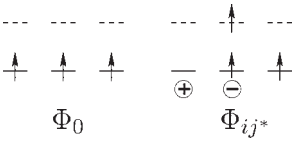

Figure 2. Schematic view of the reference function Φ_0 and the NNCT determinant Φ_{ij^*}

determinant (NNCT) Φ_{ij^*} lies $-2t$ higher in energy than Φ_O. One can easily calculate the coupling between Φ_0 and Φ_{ij^*}, $H_{ij^*} = \langle\Phi_0|\mathcal{H}|\Phi_{ij^*}\rangle = \langle i|h|j^*\rangle = t/2$. From first-order perturbation theory, the coefficient of the charge transfer determinant Φ_{ij^*} in the ground-state wavefunction $\Psi_0 = \Phi_0 + \sum c_{ij^*}\Phi_{ij^*} + \cdots$ is given by

$$c_{ij^*} = \langle\Phi_{ij^*}|\mathcal{H}|\Phi_0\rangle/2t = t/2/2t = 1/4$$

whatever the connectivity of NN bonds i and j. In the following, we shall consider systems with a single type of NNCT, that is, $c_{ij^*} = c$. However, the second-order energy correction introduces the connectivity since $2(n_c - 1)$ charge transfers between NN bonds are possible from a given i. Each charge transfer brings an energy lowering which is equal to $|H_{ij^*}|^2/2t = c_{ij^*}t/2 = t/8$. Therefore, the second-order corrected energy is

$$E^{(2)} = t + 2(n_c - 1)t/8 = t(1 + (n_c - 1)/4)$$

An improved evaluation takes into account the so-called EPV (exclusion principle violating[10]) corrections.[11] These corrections reflect the fact that acting on a given charge transfer determinant Φ_{ij^*} some similar charge transfers cannot be generated as a result of the Pauli principle. One may show that an infinite summation of the higher order corrections result in a simple energy shift of the denominators. If one calls $EPV(\Phi_K)$ the sum of the second-order corrections brought by all the excitations which are possible on Φ_0 and impossible on Φ_K, the energy denominators should be shifted according to $\Delta_{0K} = \langle\Phi_0|\mathcal{H}|\Phi_0\rangle - \langle\Phi_K|\mathcal{H}|\Phi_K\rangle \rightarrow \Delta'_{0K} = \langle\Phi_0|\mathcal{H}|\Phi_0\rangle - \langle\Phi_K|\mathcal{H}|\Phi_K\rangle - EPV(\Phi_K)$. The number of NN bonds connected to a given bond i is $2(n_c - 1)$. Since both i and j are involved and $i \rightarrow j^*$ cannot be repeated, the number of forbidden charge transfers on Φ_{ij^*} is $4n_c - 5$, while the EPV correction is $(4n_c - 5)ct/2$ (see Fig. 3). The EPV-corrected first-order coefficient therefore become connectivity dependent:

$$c = \frac{t/2}{2t + (4n_c - 5)ct/2} \qquad (1)$$

The numerical values for $n_c = 2$, 3 and 4 are given in Table 1. This leads to a second-order equation fixing an improved value as compared with 1/4 of the NNCT coefficient c and the second-order energy correction is

$$E^{(2)} = \sum_{ij^*} c\langle\Phi_{ij^*}|\mathcal{H}|\Phi_0\rangle$$

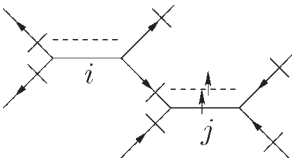

Figure 3. EPV processes in the $n_c = 3$ dendrimer. Dotted lines indicate the antibonding bond MOs i^* and j^*

Table 1. Cohesive energies of dendrimers with connectivity n_c in the unit of t

		n_c		
		2	3	4
MO-based perturbation	NNCT amplitude[a]	0.215	0.188	0.170
	2nd order	1.250	1.500	1.750
	2nd order + EPV	1.215	1.376	1.511
	4th order + EPV	1.253	1.478	1.683
AO SCPE	CT[b]	1.224	1.480	1.688
	CT/double CT[c]	1.265	1.500	1.701

[a] See Eqn (1).
[b] Self-consistent determination of the CT between adjacent atoms.
[c] Self-consistent determination of the CT and double CT between adjacent atoms.

Owing to the monoelectronic nature of the Hamiltonian $\mathcal{H}$, the third-order energy correction rises from the coupling between NNCT Φ_{ij^*} and Φ_{kl^*} with $i = k$ or $j^* = l^*$. To be non-zero, this correction requires an actual interaction between the NNCT Φ_{ij^*} and Φ_{kl^*} As will be shown later, this correction is crucial as soon as six-membered rings are present. Therefore, its contribution is strictly zero in dendrimers.

Finally, the fourth-order energy correction implies back-and-forth displacements of the electrons through charge transfer between next-nearest-neighbor (NNN) bonds. It should be noted (see the Supporting Information) that if the propagation goes through a 'branched' pattern (see Fig. 4), the contribution vanishes. The non-zero NNNCT coefficients $c^{(2)}_{ik^*}$ concern the 'linear' patterns (see Fig. 4). Since $\langle j^*|\mathcal{H}|k^*\rangle = -t/2$ and $\langle i|\mathcal{H}|k\rangle = t/2$, one obtains $c^{(2)}_{ik^*} = 2c(-t/2)/2t = -c/2$. If one introduces the EPV relative to Φ_{ik^*}, a refined evaluation of $c^{(2)}_{ik^*}$ can be derived (see Supporting Information) and the fourth-order energy correction results:

$$E^{(4)} = \sum_{ij^*}\sum_{kl^*} c\langle\Phi_{ij^*}|\mathcal{H}|\Phi_{kl^*}\rangle c$$

A self-consistent pertubative approach to the cohesive energy

A second strategy to evaluate the cohesive energy of a periodic lattice relies on a recently proposed self-consistent perturbation method[9] that we shall briefly recall here.

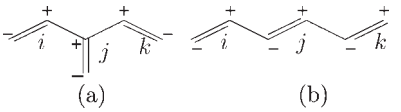

Figure 4. 'Branched' (a) and 'linear' (b) patterns of electron propagation. The signs indicate the phases on the antibonding MOs i^*, j^* and k^*

Let us start with the mostly localized picture which is based on AOs. It can be demonstrated that the valence bond determinant of largest weight in the exact wavefunction is a Néel determinant exhibiting spin alternation on all bonds. Thus, each α-electron is surrounded by β-electrons. The prevalence of this function reflects (i) the preference for neutral valence bond distribution and (ii) the impact of the Fermi hole which is due to the antisymetry of the wavefunction. If the one-site energy is arbitrarily taken as zero, the energy of Φ_0, $\langle\Phi_0|\mathcal{H}|\Phi_0\rangle$, is also zero. Starting from Φ_0, the hopping of a given electron from one site to an adjacent site gives rise to an a NNCT determinant Φ_i with positive and negative charges on the pair of atoms. For the Hückel Hamiltonian, all the valence bond distributions have the same energy, that is, zero. The exact wavefunction can be expanded in terms of the different determinants as

$$\Psi = \Phi_0 + \sum_{k\neq 0} c_k \Phi_k + \sum_{\alpha\neq 0} c_\alpha \Phi_\alpha$$

where the $\{c_k\}$ and $\{c_\alpha\}$ coefficients stand for the NNCT and beyond-NNCT amplitudes, respectively. The eigenequation problem $\mathcal{H}\Psi = E\Psi$ can be specified by simply projecting on to Φ_0. The knowledge of the NNCT amplitudes $\{c_k\}$ is sufficient to determine the energy precisely:

$$E = \sum_k c_k t$$

For equal bond lengths, the unique charge-transfer amplitude fully determines the cohesive energy $n_c ct$. The evaluation of c goes through the projection of the eigenequation problem on to the NNCT Φ_i along the i bond. The resulting equation is

$$(H_{ii} - E)c_i - H_{i0} + \sum_\alpha H_{i\alpha} c_\alpha = 0 \qquad (2)$$

where $H_{ij} = \langle\Phi_i|\mathcal{H}|\Phi_j\rangle$. Note that for a Hückel Hamiltonian the excitation energies $H_{ii} - H_{00}$ are zero, and therefore $H_{ii} - E = \sum_k c_k t$. The only determinants Φ_α interacting with Φ_i are obtained by a second charge transfer along another bond k. Provided that the reference bond i and k are sufficiently far apart, the amplitude of the Φ_α determinant can be approximated as $c_\alpha = c_k c_i = c^2$. This equation reflects the independence of the two NNCT involved in the generation of the Φ_α. For such processes, a cancellation occurs between the quantity $(-c_k t)c_i$ and the quantity $tc_k c_i$ in the first and third terms of Eqn (2). However, this particular simplification does not hold for (i) the NNCT determinants Φ_k which are not possible on Φ_i and (ii) the NNCT which generate double charge-transfer Φ_α states corresponding to non-additive excitation energies, i.e. $H_{\alpha\alpha} - H_{00} \neq H_{ii} - H_{00} + H_{kk} - H_{00}$. The former have been mentionned previously and give rise to the EPV corrections,[10] shifting the excitation energies as $\Delta'_{ii} = H_{ii} - H_{00} - EPV(i)$.[11] The amplitude c_α of the non-additive charge transfer Φ_α can be evaluated by means of first-order perturbation theory:

$$c_\alpha = c_i c_k \left(\frac{\Delta'_{ii} + \Delta'_{kk}}{\Delta'_{\alpha\alpha}}\right)$$

The difference $H_{i\alpha}c_\alpha - (c_k t_k)c_i$ in Eqn (2) vanishes as soon as $\Delta'_{ii} + \Delta'_{ii} = \Delta'_{\alpha\alpha}$. Inspection of the charge transfers along the NNN bonds of bond i displays non-additive excitation energies, $\Delta'_{\alpha\alpha} = -(4n_c - 3)ct \neq \Delta'_{ii} + \Delta'_{kk} = -2(2n_c - 1)ct$. Since the number of NNN bonds is $2(n_c - 1)^2$, the equation which determines the unique NNCT amplitude c is

$$[-(2n_c - 1)ct]c + t + \frac{2(n_c - 1)^2 tc^2}{(4n_c - 3)ct} = 0 \qquad (3)$$

The analytical resolution of this equation is obviously straightforward. More accurate evaluations can be obtained when one evaluates the coefficient d of the double-adjacent charge transfer on NNN bonds in a self-consistent manner. This strategy leads to a set of coupled equations (see Supporting Information). Interestingly, this particular treatment allows one to account for the third-order contributions which might be crucial in the characterization of cyclic effects.

A different strategy starts with bond MOs. The zeroth-order determinant Φ_0 is the product of the doubly occupied bonding MOs as in the previous perturbative approach. The charge-transfer determinants correspond to excitations $i \rightarrow j^*$ between NNN bonds. Whereas the determination of the coefficient c goes through the same logics, the cohesive energy is $t + 2(n_c - 1)ct/2 = (1 + (n_c - 1)c)t$. Since there are $2(n_c - 1)$ NNN bonds for a given one, the EPV correction to the excitation energy $-2t$ is $[4(n_c - 1) - 1]ct/2$. Using this bond MO approach, the equation defining c is

$$[-2t - (4n_c - 5)ct/2]c + t/2 + (n_c - 1)\frac{ct}{2[1 + (n_c - 1)c]} = 0 \qquad (4)$$

where the first term represents the quantity $[H_{ii} - E - EPV(i)]c$, the second is the coupling H_{0i} and the third represents the propagation effects (see Fig. 5) creating charge transfers between NNN bonds.

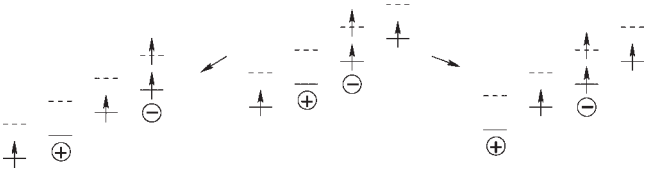

Figure 5. Schematic view of the NNN bond charge transfers

RESULTS AND DISCUSSION

Our goal was to identify the aromatic and antiaromatic contributions to the total energy of a given two-dimensional periodic systems. Considering a lattice of a given connectivity including rings, we used the same logics as before to (i) establish its cohesive energy and (ii) identify the contributions of the cyclic effects.

Evaluation of dendrimer energies

As mentioned earlier, the dendrimer energies will be used as references to identify, by contrast, the cyclic contributions of two-dimensional periodic systems which are absent in the hypothetic parent dendrimers. Both strategies based either on a step-by-step perturbative evaluation of the cohesive energy or on the so-called SCPE strategy reported previously[9] were used. As seen in Table 1, the cohesive energy increases fairly rapidly with the connectivity n_c. Therefore, in the partitioning of the energy, the connectivity has to be explicitly taken into account. Since for $n_c = 2$ the exact energy is $4/\pi \approx 1.273$, our energy calculation based on a self-consistent evaluation of both the NN and NNN charge transfer amplitudes c and d deviates by only 0.8%.

The exact energies of the 2D square lattice [$(4/\pi)^2 t = 1.621t$] and of the honeycomb lattice ($1.572t$) are known. Therefore, one may immediately estimate the cyclic corrections to be (i) stabilizing $1.57t - 1.48t = 0.09t$, $\sim$6% of the cohesive energy of the latter or (ii) destabilizing $1.62t - 1.69t = -0.07t$, $\sim$4% of the cohesive energy of the former. However, an enlightening approach consists in a direct fourth-order evaluation of the cohesive energies of these lattices, following the same expansion as those derived in the previous section. Considering a lattice of a given connectivity including rings, we used the same logics as before based on a local evaluation to establish its cohesive energy. Hence any change with respect to the corresponding dendrimer (that is, of same connectivity) can be attributed to the cyclic circulation of electrons around the ring perimeters.

In the following, special attention will be dedicated to lattices of connectivity 3 and 4. As seen in Table 1, the dispersions in the parent dendrimer energies are relatively small. Therefore, we fixed these values as references to $1.480t$ and $1.690t$, respectively.

Evaluation of honeycomb lattice energies

This strategy allows one to compare order-by-order the contributions to the energy in the graphite with respect to those in the reference 3-tree dendrimer. However, Φ_0 can be either defined from a quinonic distribution of the double bonds (i.e. all double bonds being parallel) or from a Kékulé-type distribution. For the latter, one ring over three does not hold any double bond (see Fig. 6). The zeroth- and second-order corrections are the same as for the $n_c = 3$ dendrimer. Changes appear at third-order, corrections which are absent in the dendrimer. They correspond to the processes $\Phi_0 \rightarrow \Phi_{ij^*} \rightarrow \Phi_{ik^*} \rightarrow \Phi_0$ and $\Phi_0 \rightarrow \Phi_{ij^*} \rightarrow \Phi_{kj^*} \rightarrow \Phi_0$, i.e. to a cyclic circulation of the electrons in a hexagon. The resulting third-order energy contribution is $c^2 t$. It corresponds to an anticlockwise electronic circulation. A clockwise circulation is also possible in the same hexagon and, since i belongs to two hegaxons, the third-order correction is $E^{(3)} = 4c^2 t$. The CT between NNN bonds appeared as fourth-order processes in the parent dendrimer. Consequently, there are only four remaining linear propagation to NNN bonds out of the eight in the dendrimer. The back-and-forth propagations are reduced by a factor of two. Finally, the energy change starting from the dendrimer is

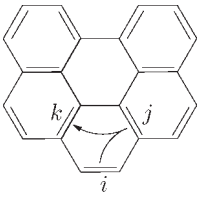

Figure 6. D_{3h} distribution of bond MOs on graphite

$$\Delta = E_{\text{graphite}} - E_{n_c=3} = 4c^2 t\left(\frac{1+4c}{2+4c}\right) = 0.094t$$

The cohesive energy of the graphite can be expressed as $E_{\text{graphite}} = (1.480 + 0.094)t = 1.574t$, which is in excellent agreement with the exact value. Therefore, the identification of the cyclic circulation of the electrons around the rings as responsible for the aromaticity of graphite is correct. They account for 6% of the cohesive energy.

An alternative approach would define either a Kékulé (see Fig. 6) or a quinonic (see Fig. 7) distribution of the double bonds (i.e. all double bonds being parallel) as a zeroth-order wavefunction to derive the SCPE. The latter strategy has been reported previously.[9] A similar identification of the circulation effects was interpreted as the enhancement of the fourth-order corrections. Indeed, the coefficient of the colinear NNNCT determinants Φ_{ik^*} is multiplied by a factor of two since it may be reached through j or j' (see Fig. 7). The processes such as $i \rightarrow j^* \rightarrow k^* \rightarrow j'^* \rightarrow i$ which do not exist in the dendrimer introduce the cyclic circulation of the electrons around the rings. Starting from the Kékulé D_{3h} symmetry

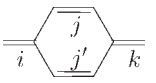

Figure 7. Quinonic distribution of the double bonds on graphite

wavefunction, the derivation of the unique SCPE is straightforward and an accurate evaluation of the NNCT amplitude which fully determines the cohesive energy can be performed. The calculated energy ($1.580t$) is again in excellent agreement with the exact value. The clockwise NNCT Φ_{ik^*} can be generated from (i) Φ_{ij^*} by propagating the electron from j^* to k^* and (ii) Φ_{jk^*} by propagating the electron from i to j (hole propagation), that is, two anti-clockwise NNCT. The resulting interference is clearly stabilizing by comparison with the $n_c = 3$ dendrimer. Hence the electronic circulation around the six-membered ring is indeed energetically favorable.

At this point, the question of the cyclic effects extension should be raised. One way to look into this important issue is to derive the SCPEs using an AO-based picture. The equation defining the unique NNCT amplitude is very similar to that given in the Supporting Information for the dendrimer. The major difference lies in the determination of the double adjacent charge-transfer amplitude when the electron jumps occur within a given six-membered ring. As pictured in Fig. 8, the electron jump on a third bond of the same ring gives rise to a third-order determinant which can actually be generated through three series of clockwise and three series of anti-clockwise jumps. The positive interference of these two series of processes introduces a cyclic circulation of the electrons that is obviously absent in the dendrimer. These processes are responsible for the energy change from the 3-tree dendrimer to the honeycomb lattice. Applying rigorously the same self-consistent method to this lattice, one has to distinguish the coefficient of the double-adjacent charge-transfer configuration in which both NNCT occur within the same ring (*cis*-movement) and the one associated with electron jumps in two different rings (*trans*-movement). The energy is calculated without any computational cost and leads to $1.574t$. Agreement with the exact value is excellent since our evaluation exhibits a negligible deviation ($<0.01\%$). Hence the aromaticity appears again as a local phenomenon induced by the cyclic circulation of the electrons around the ring perimeter.

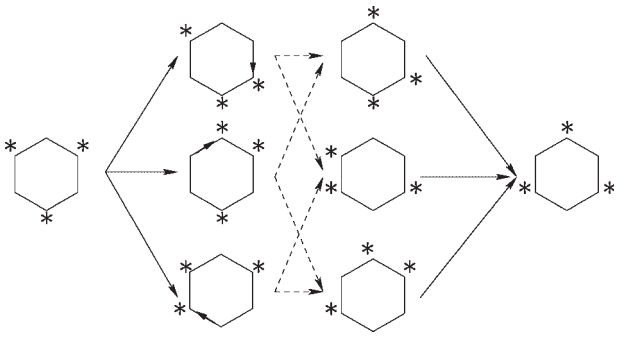

Figure 8. Clockwise processes leading to electronic circulation

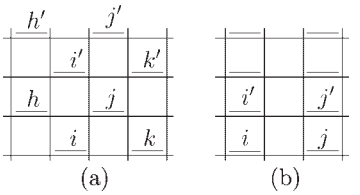

Figure 9. Bond MOs distributions on a 2D square lattice: (a) 'shifted' and (b) 'columnar'

Evaluation of 2D square lattice energy

Whether the antiaromatic effects appear as a restriction of the delocalization processes with respect to those occuring in the parent dendrimer is a relevant issue which we now intend to clarify. The reduction of the electron flow can be traced within the two so far used strategies. An appropriate zeroth-order wavefunction is pictured in Fig. 9(a). In effect, the 'columnar' wavefunction [Fig. 9(b)] does not allow any delocalization between one-dimensional horizontal chains. The electrons are constrained to move within a given horizontal line. The charge transfer $i \rightarrow i'^*$ is forbidden for symmetry reason whereas the processes $(i \rightarrow j^*)$ $(j^* \rightarrow j'^*)$ and $(i' \rightarrow j'^*)$ $(i \rightarrow i')$ cancel each other. Actually the solution converges to a solution which is merely the product of solutions on independent lines. Conversely, starting from the 'shifted' function a third-order destabilizing contribution around the square such as the clockwise circulations $(i \rightarrow j^*)$ $(j^* \rightarrow k^*)$ $(k^* \rightarrow i)$ or $(i \rightarrow j^*)$ $(k \rightarrow i)$ $(j^* \rightarrow k)$. Each of these clockwise contributions is $-c^2t/2$. By taking into account (i) the anti-clockwise contributions and (ii) the participation of i in four different rings, the total contribution is $-8c^2t$. However, the processes such as $i \rightarrow j^* \rightarrow h^* \rightarrow i$ contribute with an opposite sign, thus leading to a third-order energy-correction $E^{(3)} = -4c^2t = -0.11t$. This positive third-order effect is partly balanced by additional fourth-order corrections. For instance, the NNNCT $i \rightarrow l^*$ can be reached from $i \rightarrow j^*$ and $i \rightarrow l^*$. Moreover, one must take into account the double NNCT such as $(i \rightarrow j^*)$ $(k \rightarrow l^*)$ or such as $(i \rightarrow j'*)$ $(i' \rightarrow k'^*)$. All these additional corrections reflect the cyclic circulations along the rectangles composed of two adjacent squares. They partly compensate the destabilizing third-order effects. The antiaromatic contributions have also been investigated by means of the SCP approach. Starting from AOs, one can easily show that a pair of clockwise (or anti-clockwise) electron jumps is prohibited within the same ring. The nullity of the corresponding double charge-transfer amplitude $\Phi_{i'j'}$ is a consequence of the destructive interference between the two processes $(i \rightarrow i')$ $(j' \rightarrow j)$ and $(i \rightarrow j)$ $(j' \rightarrow i')$ (see Fig. 10). Hence the equation defining the NNCT amplitude c $(-7c^2 + 1 + 14/13c^2 = 0)$ hardly differs from that derived previously for the 4-tree $(-7c^2 + 1 + 18/13c^2 = 0)$. The cohesive energies of the 2-D square lattice and the parent dendrimer are $1.640t$

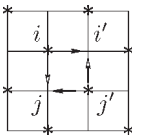

Figure 10. Destructive intereference between the up/down and right/left arrows jumps

and 1.690t, respectively. Note that the exact value is $(4/\pi)^2 t \approx 1.621t$. Hence our evaluation is (i) in good agreement with the exact value, and (ii) reflects the destabilizing contribution [(1.64–1.69) $t = -0.05t$] arising from the antiaromatic character of the 2-D square lattice.

Even though the featuring physical effects have been identified, we turned to the now usual second strategy starting from the shifted bond MOs distribution. Two types of charge transfer are to be considered, within a line ($i \rightarrow j$) and between adjacent lines ($i \rightarrow j'$). The SCPEs are easily derived. The cohesive energy of the 2D square lattice was estimated as 1.640t, in agreement with all our results.

Aromaticity versus anti-aromaticity: 2D square and hexagon containing lattices

Owing their unusual electronic and mechanical properties, hydrocarbon systems such as carbon nanotubes have attracted a great deal of interest.[12] In particular, symmetry-breaking distortions have been considered for nanotubes and also for higher dimensional compounds such as fullerenes.[13] In order to evaluate the importance of cyclic circulations, we looked into the cohesive energies of two featuring 2D squares and hexagons containing lattices, consisting of squares, hexagons and octagons. In effect, the honeycomb lattice is not the unique periodic lattice of connectivity 3.

The first periodic array we were interested is a typical structure that is encountered in zeolites such as the AlPO—5[14] (see Fig. 11). If one starts from the hexagon supported distribution of bonds, the second-order energy correction is the same as for the dendrimer since the two types of charge transfer (intra- and inter-hexagon) have the same energy and same EPV corrections. The difference appears since two out of the eight NNNCT contributions are now third-order corrections corresponding to the cyclic circulations in the hegaxon. Therefore, the comparison with the dendrimer exhibits an energy gain at third order ($2c^2t = 0.071t$) and an energy loss at fourth order [six NNNCT instead of eight, $(2c^2/(2+4c))t = 0.026t$]. Finally, the overall cyclic effects are 0.045t and account for 3% of the predicted cohesive energy, which is much less than in the graphite network (6%).

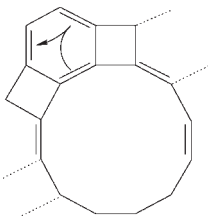

Figure 11. Schematic representation of the pseudo-zeolite array

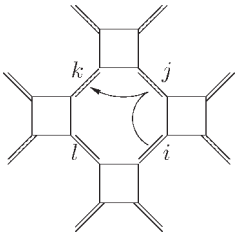

Figure 12. Schematic representation of the 1/5-depleted array

The second system is the so-called 1/5-depleted represented in Fig. 12. Such an array is well-known in theoretical solid-state physics since a magnetic lattice has been (at least for a while) schematized according to Fig. 12 in reference to the spin-gapped compound CaV_4O_9.[15] The real material is highly correlated (i.e. the bi-electronic repulsion greatly overrides the hopping integral). This particular net is also found in the non-metal part of the CaB_2C_2 system. For our purpose, one may conceive of a conjugated hydrocarbon and estimate its cohesive energy in the Hückel limit. Again, the second-order energy correction is the same as for the dendrimer. Since there is no third-order correction, the changes rise from fourth-order correction. They concern the cyclic circulation along the octagons. First, the coefficient of the NNNCT Φ_{ik^*} (see Fig. 12) is zero since Φ_0 is symmetric whereas Φ_{ik^*} is antisymmetric. This cancellation suppresses half of the fourth-order NNNCT corrections of the $n_c = 3$ dendrimer, i.e. reduces the energy by 0.051t. Then, this cancellation is partly balanced by the presence of double NNNCT such as ($i \rightarrow j^*$) ($k \rightarrow l^*$) exhibiting a charge alternation along the octagon. This state can be also reached from ($i \rightarrow j^*$), ($k \rightarrow l^*$), ($i \rightarrow l^*$) or ($k \rightarrow j^*$). Hence its coefficient (considering the exciting energy 4t and the twelve EPV) is $c_{NNN} = 4ct/2/(4t + 12ct/2) = c/(2+3c)$. This interference effect brings a stabilizing contribution of 0.014t. The overall cyclic effects are antiaromatic, $-0.051t + 0.014t = -0.037t$. However, this antiaromatic contribution is smaller than the antiaromatic contribution in the 2D square lattice.

CONCLUSION

This paper has shown, through a direct evaluation of the cohesive energy of a lattice, the fundamental roles of the connectivity and the circulation of the electrons

around the rings perimeters. The direct evaluations of the cohesive energy from localized pictures performed either from AOs or bond MOs (i.e. Kékulé determinants) are in very good agreement with exact values. By calculating the possibly EPV-corrected NNCT amplitude, we first clarified the importance of connectivity by considering dendrimeric architectures where cyclic circulations are absent. The main concept which has been conveyed is that a direct evaluation of the cyclic contributions is accessible through the cohesive energy comparison between a periodic lattice with and its parent dendrimer. The perturbative evaluation of the energy confirmed that electronic circulations are responsible for this energy difference. The energy perturbative expansion of notorious two-dimensional lattices has shed light on the relative importance of aromatic and antiaromatic contributions. Our apprach is straightforward when all the atoms in the graph have the same connectivity, but it can be generalized to any kind of lattices. Our results would be even further improved if the electron–electron repulsion which tends to localize the electrons were explicitely included. Finally, our approach might well be applied to research into cyclic effects in the σ frame. Actually, cyclic third-order effects take place in this system, in perfect isomorphism with what occurs in the π system. Such mechanisms involve, for instance, the interaction between the NNCT from the σ-bonding MO σ_{1-2} to the antibonding MO σ^*_{3-4} and the NNCT from the same bonding MO to the antibonding MO σ^*_{5-6}. Future works will extend the present analysis to more realistic treatments, and establish the connection between the energetic cyclic corrections and the magnetic properties.

REFERENCES

1. (a) Hückel E. *Z. Phys.* 1931; **70**: 204; (b) Hückel E. *Z. Phys.* 1931; **72**: 310.
2. Schleyer PvR, Jia H. *Pure Appl. Chem.* 1996; **209**: 2.
3. Shurki A, Hiberty PC, Dijkstra F, Shaik S. *J. Phys. Org. Chem.* 2003; **16**: 731–745.
4. Santos JC, Andres J, Aizman A, Fuentealba P. *J. Chem. Theory Comput.* 2005; **1**: 83–86.
5. Tour JM. *Chem. Rev.* 1996; **96**: 537–553.
6. Roncali J. *Chem. Rev.* 1997; **97**: 173–205.
7. (a) Burdett JK, Lee S. *J. Am. Chem. Soc.* 1985; **107**: 3050–3063; (b) Burdett JK, Lee S. *J. Am. Chem. Soc.* 1985; **107**: 3063–3082; (c) Burdett JK, Lee S, McLarnan TJ. *J. Am. Chem. Soc.* 1985; **107**: 3083–3089.
8. Szabo A, Ostlund NS. In *Modern Quantum Chemistry. Introduction to Advanced Electronic Structure Theory*. Dover: New York, 1996.
9. (a) Malrieu J-P, Robert V. *J. Chem. Phys.* 2004; **120**: 7374–7382; (b) Robert V, Malrieu J-P. *J. Chem. Phys.* 2004; **120**: 8853–8861.
10. Lindgren I, Morrison J. In *Atomic Many-Body Theory.* Springer: New York, 1982.
11. Daudey J-P, Heully JL, Malrieu J-P. *J. Chem. Phys.* 1993; **99**: 1240–1254.
12. Verissimo-Alves M, Capaz RB, Koiller B, Artacho E, Chacham H. *Phys. Rev. Lett.* 2001; **86**: 3372–3375.
13. Chamon CC. *Phys. Rev. B* 2000; **62**: 2806–2812.
14. Flanigen EM, Lok BM, Patton RL, Wilson ST. *Pure Appl. Chem.* 1986; **58**: 1351–1358.
15. Tanigushi S, Nishikawa T, Yasui Y, Kobayashi Y, Sato M, Nishioka T, Kontani M, Sano K. *J. Phys. Soc. Jpn.* 1995; **64**: 2758–2761.